# A chamber-integrated, axisymmetric cusp focusing system for a multi-beam heavy-ion power plant using distributed-radiator, indirect-drive targets

Grant Logan October 12, 1998

## Introduction

Debbie Callahan has recently developed smaller versions of distributed-radiator targets for heavy-ion drivers with yields of 165 MJ for 1.75 MJ of R~0.03 g/cm$^2$ ions, suitable for an IFE Engineering Test Facility (ETF), DEMO, or small power plant. However, the design requires an equivalent circular beam spot radius of 1.3 mm at the target (more than 2 x smaller than for a 5.9 MJ target), and a 12 degree half-angle constraint on the multi-beam focusing array envelopes. The small target spot and beam-array angle constraints are likely to prove difficult to meet for traditional quadrupole-focusing arrays that must be far enough back from the target to allow neutron shielding, even taking into account a factor of two smaller fusion yield per pulse, and even assuming complete plasma neutralization of beam space charge in the chamber. This preliminary note suggests that a pair of axisymmetric-cusp focusing magnets straddling the target, but with windings outside the chamber's molten-salt blanket (Fig. 1), might meet the small target spot requirement by focusing a large number of beams distributed around an annulus of ion trajectories which map into the target's annular distributed radiator. Recent hydrodynamic fluid calculations by Karani Gulec at UCLA suggest the feasibility of annular Flibe vortex flows similar to those shown in Fig. 1. This note shows that the resulting close-integration of the focusing magnets with this type Flibe-protected chamber allows an effective magnetic focal length of 1.5 meters for certain cases described below, which in turn leads to the required smaller target spots for reasonable transverse and longitudinal beam velocity spreads.

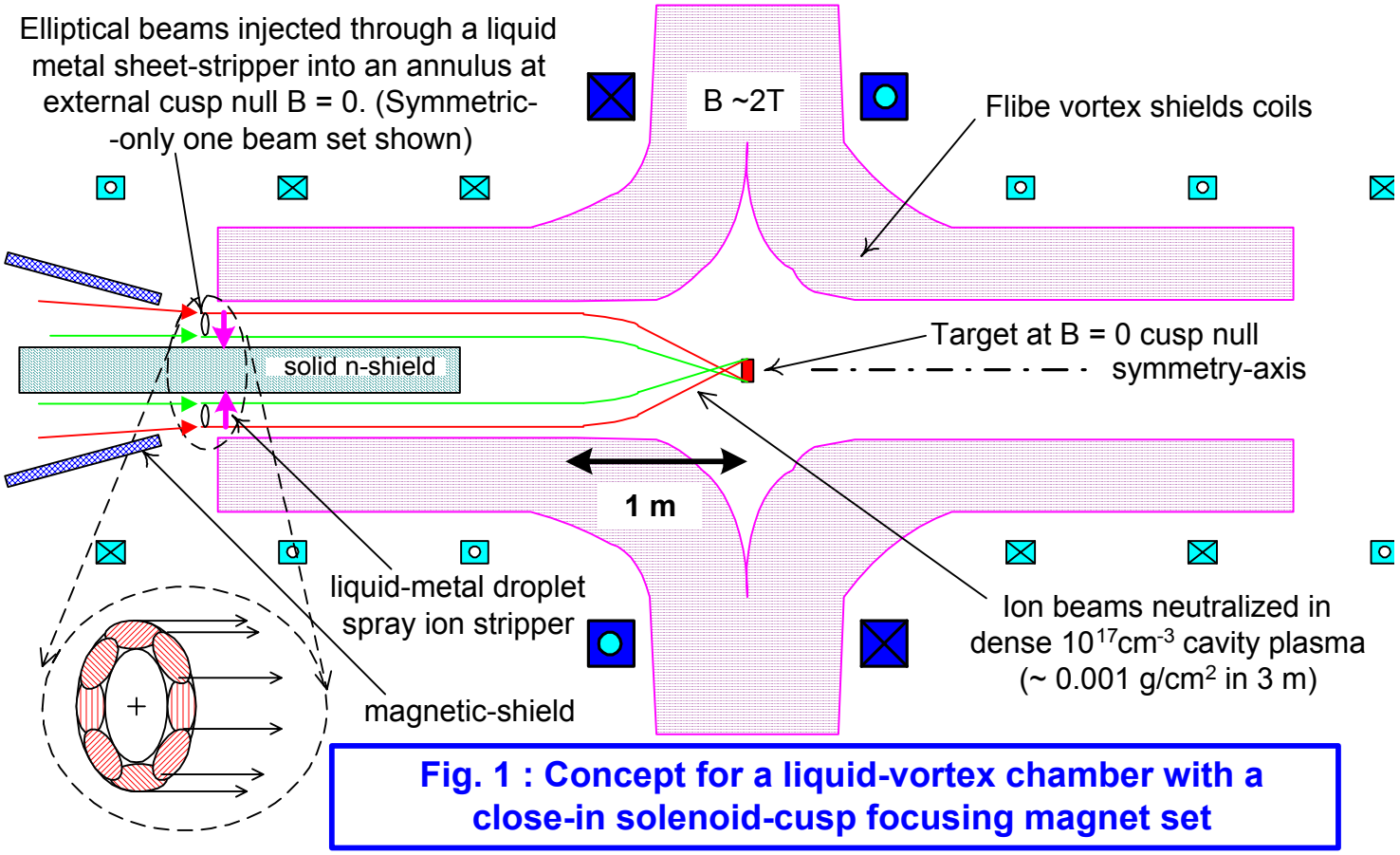


**Fig. 1 : Concept for a liquid-vortex chamber with a close-in solenoid-cusp focusing magnet set**

## Analysis

Constants

$M_p := 1.67 \cdot 10^{-27}$ (kg), the rest mass of a proton,

$e := 1.6 \cdot 10^{-19}$ (C) electron charge,

$c := 3 \cdot 10^{8}$ (m/s) the speed of light,

$m_e := 9.1 \cdot 10^{-31}$ (kg), the electron rest mass

$\varepsilon_o := 8.85 \cdot 10^{-12}$ Vacuum permittivity (Farads/m),

$\mu_o := 4 \cdot \pi \cdot 10^{-7}$ Vacuum permeability (Henrys/m)

$I_o := 3.1 \cdot 10^{7}$ (Amps) -constant in beam perveance)

$\gamma(T, A) := 1 + \frac{e \cdot T}{A \cdot M_p \cdot c^2}$ the relativistic gamma factor, with T the kinetic energy in eV, A the atomic mass number

$\beta(T, A) := \sqrt{1 - \gamma(T, A)^{-2}}$ the ion velocity normalized to c.

## Choice of ion mass and charge state for local beam propagation

While solenoids can be used as axisymmetric focusing magnets with focusing fields increasing linearly with radius (for radii small compared to the winding radii), they generally require much stronger fields than would quadrupole magnets of similar size, and that fact, together with the desire to achieve very short focal lengths with reasonable fields at the coil windings, forces the use of high-charge-state for this scheme by stripping of the incoming ions beams before entering the chamber/focusing field, whatever the ion charge state in the accelerator and drift-compression regions prior to final focus. One needs a uniform charge-state by stripping for subsequent uniform focusing, such as might be achieved by either field-ionization using short-pulse lasers, or by using foils. Experiments at the LBNL Bevalac and elsewhere with ion stripping using high-Z metal foils showed that foils can either fully strip the ions, or strip to the K-shell (helium-like ions) with negligible Rutherford scattering, as long as the ion energy per amu is high enough that a cold electron in the lab frame has enough energy to strip the desired ion bound states. For the low ion ranges considered in Debbie's targets (0.03 g/cm$^2$), we have to use ions masses below 100 to meet this condition (Lead won't fully strip, Krypton, or lower, if necessary, will strip at least to the K-shell). The required metal foil thickness are small compared to the ion range, so that the foil stripping losses are relatively small and acceptable.

The stripping "foil" can also be a source of electrons for axial beam neutralization, as Debbie Callahan and I showed was very effective in our 97 Heidelberg paper. One can use fine droplet sprays of Mercury for a power plant stripper. This scheme would be similar to the "Mini-focus" as proposed by Ed Lee, except that here we would expect, based on the Callahan/Logan Heidelberg paper, with electrons coming out of the stripper into the beam, as well as a dense residual plasma on the chamber side of the stripper, virtually 100 % neutralization of the beam current as well as space-charge. Accordingly, we would not depend on the vagarities of pinching with a particular partial beam current neutralization, but would design for ballistic focusing in the cusp field, with the spot size determined only by the beam transverse and longitudinal emmittance for a short focal length, as will be assumed in the calculations here. An advantage of this approach is that it also dispenses with the uncertainties of variable and partial strippping of ions enroute to the target, an issue that was raised again recently by Rob Goldston.

For the following calculations, we will assume double-range Krypton, with a foot at 1.2 GeV, and a main pulse at 1.7 GeV, as a compromise between accelerator and beam compression difficulty increasing with lower mass ions, and accelerator length and cost increasing with higher energy ions. The double-range is also to help ensure complete stripping, and raises the driver energy a small amount, from 1.75 MJ to 2 MJ. For Krypton, the K-edge is at 14.3 keV, with the main L-edge at 1.9 keV. A cold stripping electron has an energy in the beam frame of

$A := 83.8$ (amu) $\quad 0.5\cdot\frac{m_e}{e}\cdot\left(\beta\left(1.2\cdot10^9, A\right)\cdot c\right)^2 = 7.6\times10^3$ (eV), for the foot pulse

and $\quad 0.5\cdot\frac{m_e}{e}\cdot\left(\beta\left(1.7\cdot10^9, A\right)\cdot c\right)^2 = 1.1\times10^4$ (eV), for the main pulse.

Thus, we estimate the Krypton will strip to the K-shell,
and the charge state will be that of helium-like Krypton $q := 34$

The assumed transverse and parallel beam velocity spreads are assumed to be characterized by a normalized beam emittance and parallel momentum spread at final focus of :

$\varepsilon_{no} := 5$ ($\pi$ mm-mr) $\quad \delta p_p := 2\cdot10^{-3}$ (delta-p over p), respectively.

(Wayne's code model found solutions for the small target with $\varepsilon_{no}$ = 0.8 $\pi$ mm-mr and $\delta p_p$ = 6 x $10^{-3}$ for 192 beams of Krypton for quadrupole focusing at $L_f$ = 2 m, which has to be somehow achieved for small beams and small focusing angles of 10 milliradians. Here, the effective focusing angles are 100 milliradians, so that a higher transverse emmittance, but lower parallel spread, are tolerated). First, we calculate the cusp fields that are required at the above charge state to focus an annular pattern of foot beam pulses that enter the system nearly parallel to the axis, and then we will calculate what entrance angles will also focus the peak beams to the target at the same field.

Foot pulse ion energy $T := 1.2\cdot10^9$ (eV) $\quad \beta(T,A) = 0.173 \quad \gamma(T,A) = 1.015 \quad \delta T := 0$

To get the width of the beam spot due to parallel momentum spread, we calculate the kinetic energy spread corresponding to the given $\delta$pp:

$$\delta T_{par} := \text{root}\left(\frac{\gamma\left(T+\delta T, A\right)\cdot\beta\left(T+\delta T, A\right)}{\gamma(T,A)\cdot\beta(T,A)} - 1 - \delta p_p, \delta T\right) \qquad \delta T_{par} = 4.77\times10^6 \quad \text{(eV)}$$

The normalized emittance can be expressed in terms of a transverse ion temperature $\Delta T_x$ :

$$\varepsilon_n\left(T, \Delta T_x, A, a_f\right) := 2\cdot\gamma(T,A)\cdot a_f\cdot\sqrt{\frac{e\cdot\Delta T_x}{A\cdot M_p\cdot c^2}}\cdot10^6 \quad (\pi \text{ mm-mr}),$$

where $\Delta T_x$ (in eV) is measured at the beam radius $a_f$ just before the final focus lens. The factor of $10^6$ is inserted so that the normalized emittance can be expressed in the usual units of millimeters times milliradians. This equation can be solved for the allowed $\Delta T_x$ for a given normalized emmittance $\varepsilon_n$ and input beam minor radius $a_f$ , with ellipticity ell at final focus:

$ell := 3 \quad a := 5\cdot10^{-2}$ (m) $\quad a_f := \sqrt{ell}\cdot a \quad \Delta T_x := \left(\frac{\varepsilon_{no}}{2\cdot10^6\cdot\gamma(T,A)\cdot a_f}\right)^2\cdot A\cdot\frac{M_p}{e}\cdot c^2$

$\Delta T_x = 63.64$ (eV)

The corresponding transverse radial velocity $vr_x$ and angular spread $\theta_x$ at the input to the final focus is

$$vr_x := \sqrt{\frac{2\cdot e\cdot \Delta T_x}{A\cdot \gamma(T,A)\cdot M_p}} \qquad vr_x = 1.197\times 10^{4} \quad \text{(m/s)} \qquad \theta_x := \frac{vr_x}{\beta(T,A)\cdot c} \qquad \theta_x = 2.312\times 10^{-4}$$

(radians)

We will use these velocity and angular spreads on test ion to characterize the beam spot envelope size on target. For the fields, we use the familiar paraxial approximation to get the $B_z$ and $B_r$ components (in MKS units- tesla): (future work can use exact fields taken from elliptic integrals, but those won't likely change the basic orbits much after a little tweaking for off-axis ion injection).

$$Bz(I,a,x,z) := \frac{\mu_o\cdot I}{2}\cdot\frac{a^2}{\left[a^2+(z-x)^2\right]^{1.5}} \qquad Br(I,a,r,x,z) := \frac{3\cdot\mu_o\cdot I}{4\cdot a}\cdot\left[\frac{r\cdot(z-x)}{a^2}\right]\cdot\left[1+\left(\frac{z-x}{a}\right)^2\right]^{-2.5}$$

where "a" is the radius of an assumed winding cross-section (filamentary current approximation) at a z-location "x" for a given coil. To simplify the determination of coil currents which can bend chosen ion trajectories into the target, we take a set of coils symmetric about the z=0 target location, and we make the innermost and outermost pairs of coil currents opposing so as to create a cusp null at the chosen injection plane as well as at the target center. Thus, we inject ions with zero canonical angular momentum into the focusing system, so that ion orbits can pass through the r=0 axis:

$mc := 0.26023\cdot\frac{36}{34}$ This current multiplier is adjusted to focus the ions on target after crossing.

$I_1 := mc\cdot 15\cdot 10^6$ $a_1 := 1.5$ $x_1 := -0.75$ $I_3 := mc\cdot 3\cdot 10^6$ $a_3 := 1$ $x_3 := -1.5$

$I_2 := -mc\cdot 15\cdot 10^6$ $a_2 := 1.5$ $x_2 := 0.75$ $I_4 := -mc\cdot 3\cdot 10^6$ $a_4 := 1$ $x_4 := 1.5$

$I_5 := mc\cdot 1\cdot 10^6$ $a_5 := 1$ $x_5 := -2.5$ $I_7 := -mc\cdot 3\cdot 10^6$ $a_7 := 1$ $x_7 := -3.5$

$I_6 := -mc\cdot 1\cdot 10^6$ $a_6 := 1$ $x_6 := 2.5$ $I_8 := mc\cdot 3\cdot 10^6$ $a_8 := 1$ $x_8 := 3.5$

The field at any point along the ion trajectory (in the paraxial approximation), is given by summing the contributions of the eight coils specified above:

$$B_z(z) := \sum_{nc=1}^{8} Bz\left(I_{nc},a_{nc},x_{nc},z\right) \qquad B_r(r,z) := \sum_{nc=1}^{8} Br\left(I_{nc},a_{nc},r,x_{nc},z\right)$$

By iteration using the above $B_z(z)$ we determine the initial injection plane $z_o$ (where the ion stripper jet is placed at the outside entrance cusp null):

$B_z(-3.047278) = -6.26\times 10^{-8}$ (T) $z_o := -3.047278$ (m)

We run seven test ion orbits: the first three without either transverse or longitudinal velocity spread, starting at the outer radius, the midpoint, and the inner radius of the injection annulus. The fourth and fifth test ions have the + and - parallel momentum corresponding to the assumed $\delta p/p$, and the sixth and seventh test ions have the same $\delta p/p$ spread plus the transverse spread corresponding to the assumed normalized emittance of the beams. The indici "j" will denote each ion orbit case.

For $j := 1 .. 7$ test orbits, we define intitial injection radii (in meters)

$ro_1 := 0.3$ $ro_2 := 0.25$ $ro_3 := 0.2$ $ro_4 := ro_2$ $ro_5 := ro_2$ $ro_6 := ro_2$ $ro_7 := ro_2$

The corresponding intial canonical angular momenta are zero, and this is preserved in the orbits; e.g,

$$P\theta_j := 0.5 \cdot q \cdot e \cdot B_z(z_o) \cdot (ro_j)^2$$

$P\theta_1 = 0$ $P\theta_7 = 0$

The initial angles are iterated for the first three principle orbits (without the velocity spreads), starting with zero as an initial guess, to bring all three principle rays into focus at Debbies target radiator annulus:

$\theta o_1 := .1 \cdot 10^{-4}$ $\theta o_2 := 18 \cdot 10^{-4}$ $\theta o_3 := 27 \cdot 10^{-4}$ <-principle rays start ~parallel to the axis for the foot.

$\theta o_4 := \theta o_2$ $\theta o_5 := \theta o_2$ <-these two have only the parallel spread added

$\theta o_6 := \theta o_2 - \theta_x$ $\theta o_7 := \theta o_2 + \theta_x$ <-these two have both transverse and parallel spreads added

$To_1 := T$ $To_2 := T$ $To_3 := T$ <-principle ion orbits = foot energy

$$To_4 := T + \frac{\delta T_{par}}{2} \qquad To_5 := T - \frac{\delta T_{par}}{2}$$ <- parallel velocity spread added

$$To_6 := T + \frac{\delta T_{par}}{2} + \Delta T_x \qquad To_7 := T - \frac{\delta T_{par}}{2} - \Delta T_x$$ <-parallel + transverse spreads added

$vro_j := -\sin(\theta o_j) \cdot \beta(To_j, A) \cdot c$ $vzo_j := \cos(\theta o_j) \cdot \beta(To_j, A) \cdot c$ <-corresponding initial orbit radial and axial velocities

With these above selected seven ion initial conditions, we next integrate the radial force = q $v_\theta$ x $B_z$ on each ion orbit through the cusp focusing system, using the local $v_\theta$ derived from conservation of canonical angular momentum.

$k_{max} := 2000$ For $k := 1 .. k_{max}$ steps $\delta z := 2 \cdot |z_o| \cdot k_{max}^{-1}$ $\delta z = 3.05 \times 10^{-3}$ (m)

$$\begin{pmatrix} r_{1,j} \\ z_1 \\ t_{1,j} \\ vr_{1,j} \\ v\theta_{1,j} \\ vz_{1,j} \end{pmatrix} := \begin{pmatrix} ro_j \\ z_o \\ 0 \\ vro_j \\ 0 \\ vzo_j \end{pmatrix}$$

Initial conditions for each test ion is set by MathCAD

Then each j = 1 ..7 ion test orbits are calculated for k-steps through the focusing system:

$$\begin{pmatrix} r_{k+1,j} \\ z_{k+1} \\ t_{k+1,j} \\ vr_{k+1,j} \\ v\theta_{k+1,j} \\ vz_{k+1,j} \end{pmatrix} := \begin{bmatrix} r_{k,j} + vr_{k,j} \cdot \dfrac{\delta z}{vz_{k,j}} \\ z_k + \delta z \\ t_{k,j} + \dfrac{\delta z}{vz_{k,j}} \\ vr_{k,j} + \dfrac{q \cdot e \cdot v\theta_{k,j} \cdot B_z(z_k)}{A \cdot M_p \cdot \gamma(To_j, A)} \cdot \dfrac{\delta z}{vz_{k,j}} \\ \dfrac{P\theta_j - 0.5 \cdot q \cdot e \cdot B_z(z_k) \cdot (r_{k,j})^2}{\gamma(To_j, A) \cdot A \cdot M_p \cdot r_{k,j}} \\ \beta\left[ To_j - \dfrac{\gamma(To_j, A)}{2 \cdot e} \cdot M_p \cdot A \cdot \left[ (vr_{k,j})^2 + (v\theta_{k,j})^2 \right], A \right] \cdot c \end{bmatrix}$$

F=Ma radial force equation gives $v_r$

$v_\theta$ obtained from $P\theta$

total ion energy conservation

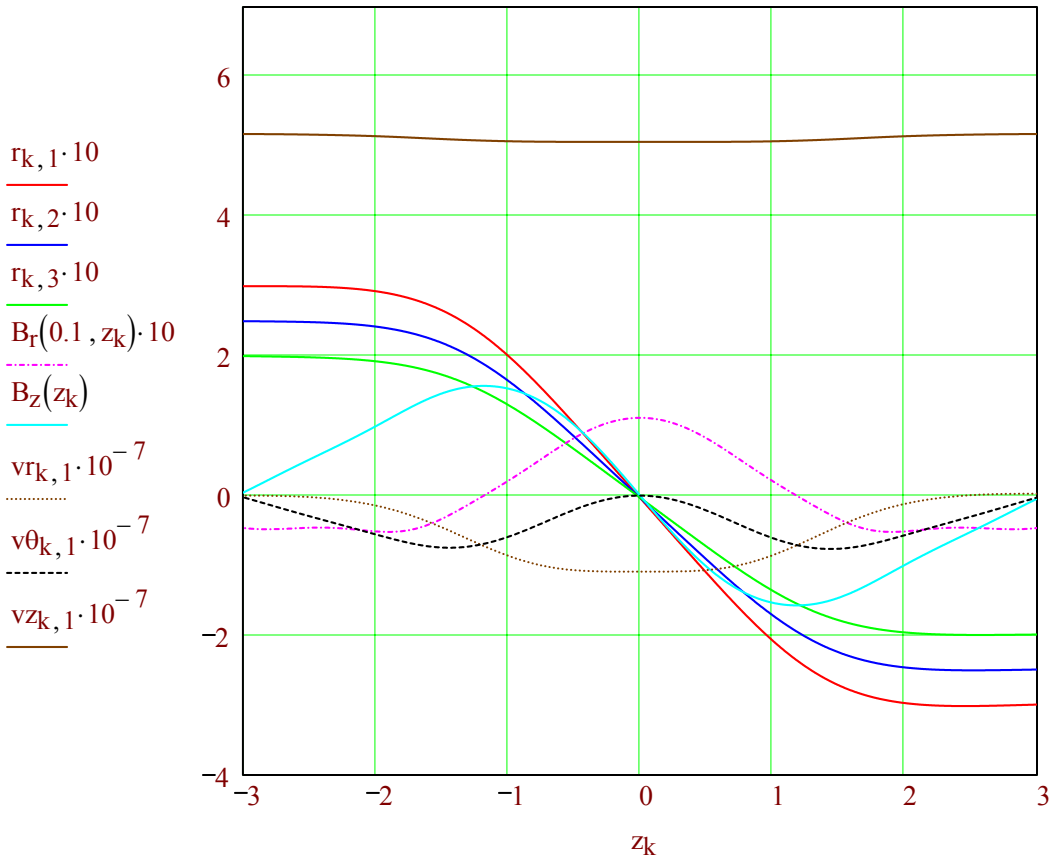


Krypton

$T = 1.2 \times 10^9$ (eV)

(Foot pulse)

$q = 34$

Charge-state

distance along axis z

Fig. 2 Plots of principle orbits through the focusing system shown in Fig. 1. The fields and velocities exhibit the expected symmetry properties of the conservation laws. Note the radial scale is magnified 5 x with respect to the z-axis. (Foot pulse). $B_z$ ~ 1.6 T cusp fields required at q =34.

Next, we replot the above orbits with greater magnification around the target ceter at r=0, z=0.

$k := 990 .. 1005$

Holraum lines: $bbr_k := 600\cdot\Phi(998 - k) - 1.6\cdot\left[1 + 0.33\cdot(k - 999)\cdot\Phi(k - 999)\right]\cdot\Phi(k - 999)$

$hir_k := 600\cdot\Phi(998 - k) - 2.8\cdot\left[1 + 0.19\cdot(k - 999)\cdot\Phi(k - 999)\right]\cdot\Phi(k - 999)$

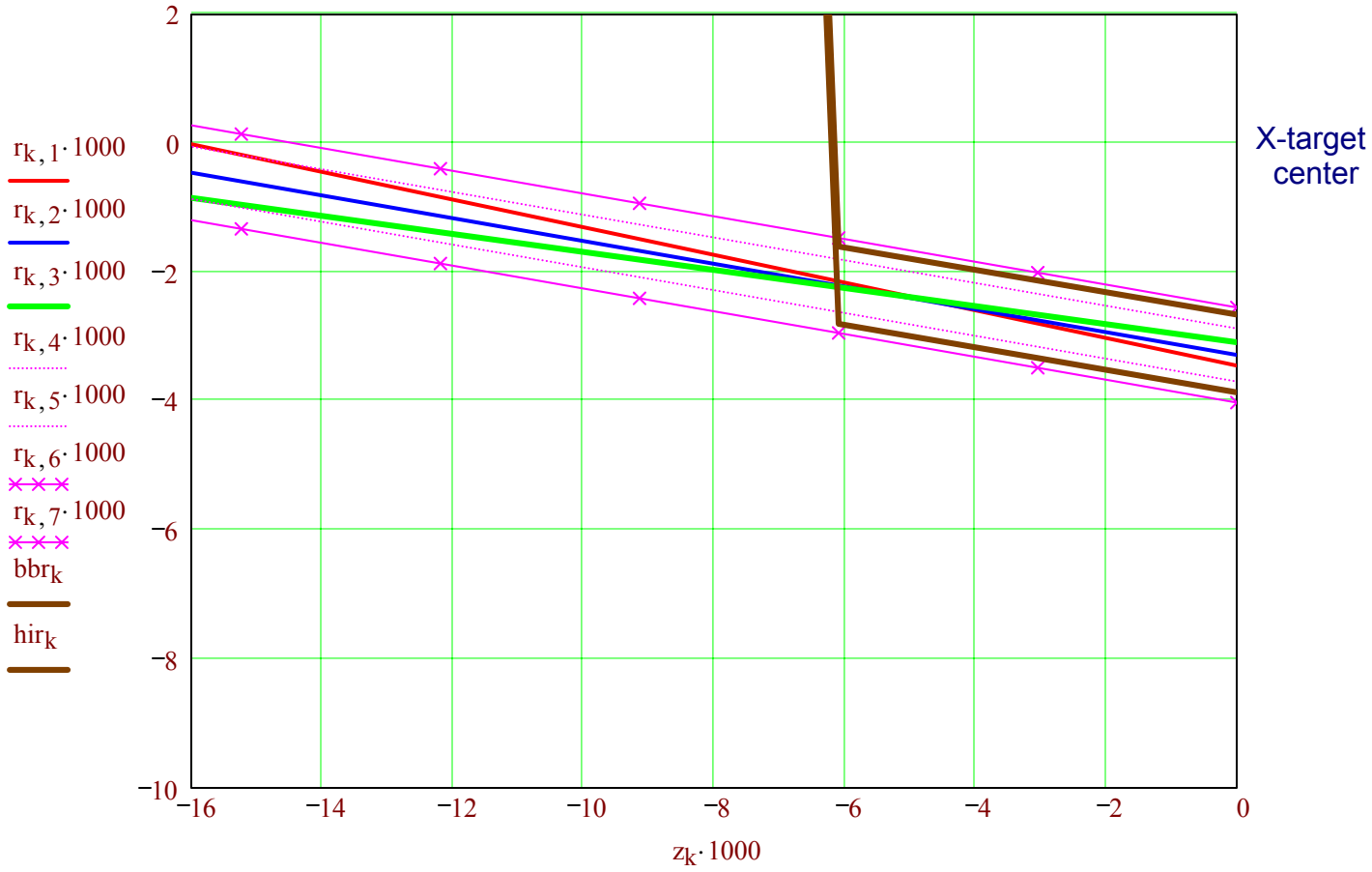


Fig. 3. The foot-ion orbits are now plotted on a mm-scale with equal radial and axial magnifications, distances in millimeters. The outlines of the hohlraum showing the approximate beam-block and conical-radiator sections are superimposed to show how the three principle rays (red, blue and green) are first focused onto the target radiator annulus by adjusting the cusp field and the initial (near-parallel) ion injection angles. The effect of adding the parallel momentum spread is shown by the dotted line about the central blue ray, and the effect of combined parallel and transverse velocity spread is shown by the lines with x's. All representative ions should fill-in this maximum envelope. (Foot-pulse orbits)

Next, we find a different set of initial injection angles into the same B=O injection annulus, such that the peak ions would also focus to the same target annulus with the same cusp fields used for the foot:

At peak pulse, $T := 1.7 \cdot 10^9$ (eV) $\beta(T, A) = 0.205$ $\gamma(T, A) = 1.022$ $\delta T := 0$

The paralle energy spread for the same $\delta p_p$ in the peak is

$$\delta T_{par} := \text{root}\left(\frac{\gamma(T + \delta T, A) \cdot \beta(T + \delta T, A)}{\gamma(T, A) \cdot \beta(T, A)} - 1 - \delta p_p, \delta T\right) \qquad \delta T_{par} = 6.74 \times 10^6 \quad \text{(eV)}$$

$$\Delta T_x := \left(\frac{\varepsilon_{no}}{2 \cdot 10^6 \cdot \gamma(T, A) \cdot a_f}\right)^2 \cdot A \cdot \frac{M_p}{e} \cdot c^2 \qquad \Delta T_x = 62.86 \quad \text{(eV)}$$

The corresponding transverse radial velocity $vr_x$ and angular spread $\theta_x$ at final focus are

$$vr_x := \sqrt{\frac{2 \cdot e \cdot \Delta T_x}{A \cdot \gamma(T, A) \cdot M_p}} \qquad vr_x = 1.186 \times 10^4 \quad \text{(m/s)} \qquad \theta_x := \frac{vr_x}{\beta(T, A) \cdot c} \qquad \theta_x = 1.933 \times 10^{-4}$$

(radians)

The stripping electron energy for the peak $0.5 \cdot \frac{m_e}{e} \cdot (\beta(T, A) \cdot c)^2 = 1.1 \times 10^4$ (eV)

...is still below the Krypton K-shell, so $q = 34$ as in the foot.

The initial angles are iterated again for the first three principle orbits (without the velocity spreads), now larger angles pointing to the target to bring all three principle rays into focus at the same target radiator annulus for the higher peak energy in the same magnetic fields

$\theta o_1 := 4.25 \cdot 10^{-2}$ $\theta o_2 := 3.61 \cdot 10^{-2}$ $\theta o_3 := 2.942 \cdot 10^{-2}$ <-principle rays now point to the axis for the higher energy peak ions, because now the same cusp field bends the higher energy peak ions less than for the foot.

$\theta o_4 := \theta o_2$ $\theta o_5 := \theta o_2$ <-these two have only the parallel spread added

$\theta o_6 := \theta o_2 - \theta_x$ $\theta o_7 := \theta o_2 + \theta_x$ <-these two have both transverse and parallel spreads added

$To_1 := T \quad To_2 := T \quad To_3 := T$ <-principle ion orbits = peak energy $T = 1.7 \times 10^9$ (eV)

$To_4 := T + \frac{\delta T_{par}}{2} \quad To_5 := T - \frac{\delta T_{par}}{2}$ <- parallel velocity spread added

$To_6 := T + \frac{\delta T_{par}}{2} + \Delta T_x \quad To_7 := T - \frac{\delta T_{par}}{2} - \Delta T_x$ <-parallel + transverse spreads added

$vro_j := -\sin(\theta o_j) \cdot \beta(To_j, A) \cdot c \quad vzo_j := \cos(\theta o_j) \cdot \beta(To_j, A) \cdot c$ <-corresponding initial orbit radial and axial velocities

With these above selected seven ion initial conditions for the peak pulse, we next again integrate the radial force = q $v_\theta$ x $B_z$ on each ion orbit through the cusp focusing system, using the local $v_\theta$ derived from conservation of canonical angular momentum.

$k_{max} := 2000$ For $k := 1 .. k_{max}$ steps $\delta z := 2 \cdot |z_o| \cdot k_{max}^{-1} \quad \delta z = 3.05 \times 10^{-3}$ (m)

$$\begin{pmatrix} r_{1,j} \\ z_1 \\ t_{1,j} \\ vr_{1,j} \\ v\theta_{1,j} \\ vz_{1,j} \end{pmatrix} := \begin{pmatrix} ro_j \\ z_o \\ 0 \\ vro_j \\ 0 \\ vzo_j \end{pmatrix}$$

Initial conditions for each test ion is set by MathCAD

Then each j = 1 ..7 ion test orbits are re-calculated for the peak ion energy and initial injection angles for k-steps through the focusing system:

$$\begin{pmatrix} r_{k+1,j} \\ z_{k+1} \\ t_{k+1,j} \\ vr_{k+1,j} \\ v\theta_{k+1,j} \\ vz_{k+1,j} \end{pmatrix} := \begin{bmatrix} r_{k,j} + vr_{k,j}\cdot\dfrac{\delta z}{vz_{k,j}} \\ z_k + \delta z \\ t_{k,j} + \dfrac{\delta z}{vz_{k,j}} \\ vr_{k,j} + \dfrac{q\cdot e\cdot v\theta_{k,j}\cdot B_z(z_k)}{A\cdot M_p\cdot\gamma(To_j, A)}\cdot\dfrac{\delta z}{vz_{k,j}} \\ \dfrac{P\theta_j - 0.5\cdot q\cdot e\cdot B_z(z_k)\cdot(r_{k,j})^2}{\gamma(To_j, A)\cdot A\cdot M_p\cdot r_{k,j}} \\ \beta\left[To_j - \dfrac{\gamma(To_j, A)}{2\cdot e}\cdot M_p\cdot A\cdot\left[(vr_{k,j})^2 + (v\theta_{k,j})^2\right], A\right]\cdot c \end{bmatrix}$$

F=Ma radial force equation gives $v_r$

$v_\theta$ obtained from $P\theta$

total ion energy conservation

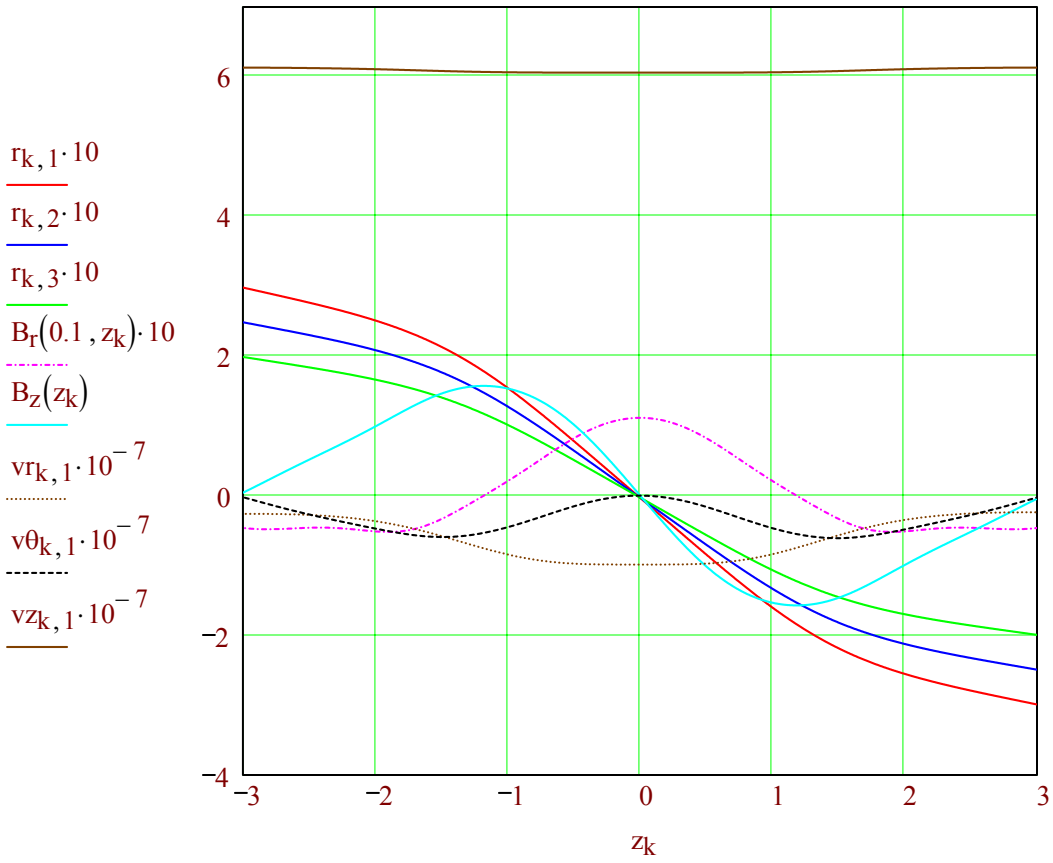


Krypton

$T = 1.7 \times 10^9$ (Peak pulse)

$q = 34$

Charge-state

distance along axis z

Fig. 4 Plots of principle orbits through the focusing system shown in Fig. 1 for the peak ion energy. Note now that the injection angles point toward the target since the same cusp fields bend the higher energy peak ions less than the previous foot-pulse ions. Same plot scales as in Fig. 2. Same $B_z$ ~ 1.6 T cusp fields required at same q =34.

Next, we replot the above orbits with greater magnification around the target ceter at r=0, z=0

$k := 990 .. 1005$

Holraum lines: $bbr_k := 600\cdot\Phi(998 - k) - 1.6\cdot\left[1 + 0.33\cdot(k - 999)\cdot\Phi(k - 999)\right]\cdot\Phi(k - 999)$

$hir_k := 600\cdot\Phi(998 - k) - 2.8\cdot\left[1 + 0.19\cdot(k - 999)\cdot\Phi(k - 999)\right]\cdot\Phi(k - 999)$

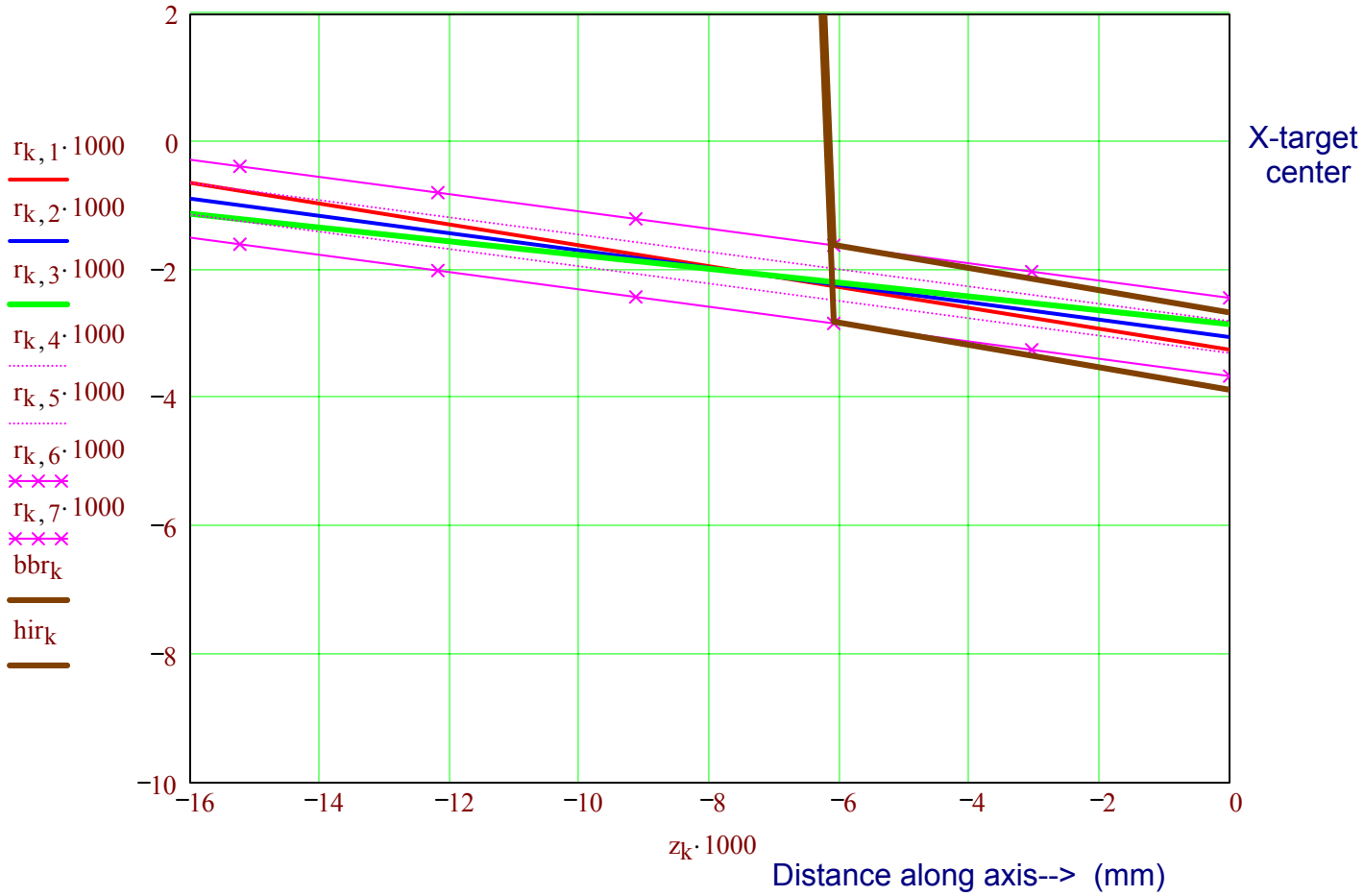


Fig. 5. The peak-ion orbits corresponding to the injection angles shown in Fig. 4 are now plotted on the same mm-scale as in Fig. 3. The outlines of the same hohlraum are shown again with the approximate beam-block and conical-radiator sections superimposed to show how the three principle rays (red, blue and green) (now at the peak ion energy) are first focused onto the target radiator annulus by adjusting only the initial injection angles as shown in Fig. 4. The effect of adding the parallel momentum spread is shown by the dotted line about the central blue ray, and the effect of combined parallel and transverse velocity spread is shown by the lines with x's. All representative peak ions should fill-in this maximum envelope. This shows how Callahan's target requirements for different foot and peak beam energies can be brought to a common focus at the target, by having a circle of peak beams at larger radius around a ring of foot-pulse beams shooting at the same injection annulus in this focusing scheme. This would put the end of the beam compression transport lines a few meters further to the left of Fig. 1. Space-charge effects should be tolerable for injection across such a space into the ion stripper jey and cavity plasma, since each beam footprint is allowed to be an ellipse as large as 30 x 10 centimeters (for this example).

## Discussion and future research

There are many implications of this memo that need to be explored, including:
(1) attempt a preliminary layout of a conventional quadrupole focusing array for this small target, at least to the same level as this memo--with neutron shielding interfaces, partial beam space-charge neutralization and stripping effects with deep-shell ionization included, to see if we really need to look at alternative focusing schemes like this one in order to exploit Callahan's small target.
(2) redo these caculations using exact fields without the paraxial approximation, to check the effect of radial non-linearities at injection radii of 10 to 30 % of the coil radii--see if the coil radii have to be increased, or if the injection angles can be tweaked to compensate for such non-linear radial field components.
(3) a beam transport and injection design to get as many as perhaps 50-100 beams injected into the annular pattern as suggested in Fig. 1. Care has to be taken to shield out any stray fields between the end of the beam compression transport lines and the first low field cusp null, to avoid non-zero $P\theta$ affecting the beam radial convergence near the target. Evaluate effects of small but non-zero $v\theta$ components due to practical injected beam geometry from the transport lines.
(4) review the metal foil stripping data and theoretical models for stripping of ions in condensed-phase metals, for the medium-heavy ions in the 20 MeV per amu regime for HIF, to determine more precisely the uniformity of charge states that are possible, or to determine at what lower mass ion than Krypton would ions be assuredly fully stripped. Estimate Rutherford scattering in the stripping process to check its significance.
(5) look for models like IPROP to check that beam current as well as charge neutralization is complete, in this situation in which significant residual Flibe vapor hangs around somewhat magnetised in the chamber between shots due to the cusp field (see further discussion below).

## Other implications of this chamber scheme to be explored

Since the fusion yield of 165 MJ with this small target is less than half that assumed for HYLIFE-II, while the liquid pocket radius can be twice as large as HYLIFE-II, it is possible that this example, or one slightly modified, if necessary, with a somewhat larger vortex radius, will result in the elimination of isochoric bulk liquid break-up due to neutron energy deposition being reduced an order of magnitude. If one can then also limit the amount of cold Flibe vapor that is ablated-off the liquid surface from target debris and x-rays, the surface shocks may be mitigated to the point that there is no re-bound surface "lift-off" under the 10-g artifical gravity created by the vortex (Gulac-UCLA calculations, discussions with Ralph Moir), there may no longer be any liquid droplets or splash to clear in the pocket between shots, just some very hot, relatively low density, ionized Flibe vapor decaying by radiation cooling and flow along the field lines out the ends of the two external cusps. Note that the strong cusp field in Fig. 1 should be MHD stable (please forgive the use of an MFE-term) to confine target-debris plasma, in the short-term sense of retarding direct ablation of the Flibe liquid vortex surface by the target debris plasma. If the target hohlraum wall, which Ralph proposes to make from frozen Flibe castings coated with hi-Z, were made of order 1-cm thick, then one can show that the x-ray output spectrum is downshifted from several hundred eV down to perhaps 10's of eVs. This would lead to greatly reduced Flibe masses ablated from the vortex surface, as well as hotter, even ionized Flibe vapor, with much reduced momemtum impluse and weakened ablation shocks. *This may eliminate the need for forced-displacement clearing of the pocket, and since the thick frozen-Flibe hohlraum casings can survive injection into the dense 10 eV chamber plasma, there may also be no need to fully extinguish the chamber plasma between shots back to vacuum. This raises the far-reaching prospect of very-high pulse-rate capability for this type of chamber, perhaps up to 30-60 Hz, as well as to other possibilities*